



HAL
open science

An Analytic Geometry Approach to Wiener System Frequency Identification

Fouad Giri, Youssef Rochdi, Fatima Zara Chaoui

► **To cite this version:**

Fouad Giri, Youssef Rochdi, Fatima Zara Chaoui. An Analytic Geometry Approach to Wiener System Frequency Identification. IEEE Transactions on Automatic Control, 2009, 54 (4), pp.683-696. 10.1109/TAC.2009.2014915 . hal-01058103

HAL Id: hal-01058103

<https://hal.science/hal-01058103v1>

Submitted on 11 Jul 2022

HAL is a multi-disciplinary open access archive for the deposit and dissemination of scientific research documents, whether they are published or not. The documents may come from teaching and research institutions in France or abroad, or from public or private research centers.

L'archive ouverte pluridisciplinaire **HAL**, est destinée au dépôt et à la diffusion de documents scientifiques de niveau recherche, publiés ou non, émanant des établissements d'enseignement et de recherche français ou étrangers, des laboratoires publics ou privés.



Distributed under a Creative Commons Attribution - NonCommercial 4.0 International License

An Analytic Geometry Approach to Wiener System Frequency Identification

Fouad Giri, *Member, IEEE*, Youssef Rochdi, and Fatima-Zahra Chaoui

Abstract—This paper addresses the problem of Wiener system identification. The underlying linear subsystem is stable but not necessarily parametric. The nonlinear element in turn is allowed to be nonparametric, noninvertible, and nonsmooth. As Wiener models are uniquely defined up to an uncertain multiplicative factor, it makes sense to start the frequency identification process estimating the system phase (which is common to all models). To this end, a consistent estimator is designed using analytic geometry tools. Accordingly, the system frequency behavior is characterized by a family of Lissajous curves. Interestingly, all these curves are candidates to modelling the system nonlinearity, but the most convenient one is the less spread of them. Finally, the frequency gain is in turn consistently estimated optimizing an appropriate cost function involving the obtained phase and nonlinearity estimates.

Index Terms—Frequency identification, Lissajous curves, nonlinear block-oriented systems, system identification, Wiener systems.

I. INTRODUCTION

THE Wiener model consists of a linear dynamic subsystem followed in series by a nonlinear element (Fig. 1). Most of previous identification methods were developed supposing that the nonlinearity is a polynomial of known degree and the linear part is a transfer function of known order, see e.g., [11], [13]–[15], [17], [19]. As the intermediate signal $x(t)$ is not accessible for measurement (and may even be of no physical meaning), the system output then turns out to be a bilinear (but fully known) function of the unknown parameters (those of the nonlinearity and those of the linear subsystem). Such bilinearity has been coped with following different approaches. First, the iterative optimization method consists in computing alternatively the parameters of the linear subsystem and those of the nonlinear subsystem. When optimization is performed with respect to one set of parameters, the other set is fixed. Such a procedure is shown to be efficient provided that it converges, e.g., [17]. But, convergence can not be achieved except under restrictive conditions, e.g., [20]. In [3], a separable nonlinear optimization solution is suggested. It consists in expressing a part of the parameters (namely, those of the linear subsystem) in function of the others, using first order optimality conditions. The dimension of the parameter space is thus reduced making

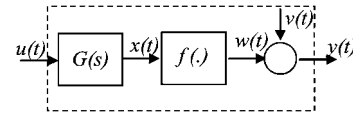


Fig. 1. Wiener model structure.

easier the optimization problem. Frequency-type solutions have also been proposed, see e.g., [6]. The idea is to apply repeatedly a sine input $u(t) = U_k \cos(\omega_k t)$ with different amplitudes U_k and frequencies ω_k . Then, exploiting the polynomial nature of the nonlinearity, the input-output equation can be solved with respect to the unknown parameters.

Nonparametric nonlinearities have also been dealt with using different approaches. In [7]–[10], the identification problem was dealt with using stochastic tools. But, the nonlinearity is supposed to be invertible and smooth. In [1] a frequency method is proposed for noninvertible nonlinearities. It consists in applying repeatedly sine input signals and operating a discrete-Fourier transformation of the obtained (steady-state) periodic output signals to estimate the frequency gain $G(j\omega_k)$ (for different frequencies) and the nonlinearity. Unfortunately, the proposed estimators (phase, gain and nonlinearity) are not consistent in general as this is pointed out in [2]. A stochastic solution has been proposed in [12], where the linear subsystem coefficients are first estimated using a least-squares type algorithm and the obtained estimates are used to recover the nonlinearity $f(x)$ at any fixed x . The consistency is established supposing that the linear subsystem is MA with known and nonzero leading coefficient. The nonlinearity was assumed to be continuous with growth not faster than a polynomial. In [5], a recursive identification scheme is proposed for Wiener systems including a dead-zone preload nonlinearity. There too, consistency is only achieved supposing the linear subsystem to be MA with known and nonzero leading coefficient. More recently, a semi-parametric identification approach has been presented in [16]. The impulse response function of the linear subsystem is identified via the nonlinear least squares approach with the system nonlinearity estimated by a pilot nonparametric kernel regression estimate. The linear subsystem estimate is then used to form a nonparametric kernel estimate of the nonlinearity. The price paid is that the impulse response function is truncated to a finite order which, in effect, amounts to suppose the linear subsystem to be MA.

In this paper, a new frequency-domain identification scheme is designed for Wiener systems involving possibly noninvertible and nonsmooth nonlinearities. The identification purpose is to estimate the system nonlinearity $f(\cdot)$ and the system phase and gain ($\angle G(j\omega_k)$, $|G(j\omega_k)|$), for a set of a priori chosen frequencies ω_k ($k = 1, \dots, m$). As a matter of fact, the

F. Giri is with the Groupe de Recherche en Informatique, Image, Automatique, Instrumentation de Caen (GREYC) Laboratory, University of Caen Basse-Normandie, Caen 14032, France (e-mail: fouad.giri@unicaen.fr).

Y. Rochdi and F.Z. Chaoui are with the LAII, EMI, Rabat, Morocco and also with the Department of Electrical Engineering, L'Ecole Supérieure de l'Enseignement Technique (ENSET), Rabat, Morocco (e-mail: youssef-rochdi@yahoo.fr, chaouifatima@yahoo.fr).

estimation of the linear subsystem (gain and phase) is much more complex in the case of noninvertible nonlinearities. The complexity arises from the fact that the (unavailable) internal signal $x(t)$ cannot be uniquely reconstituted from the output signal. Consequently, the system cannot be uniquely modelled i.e., any couple of the form $(G(s)/K, f(Kx))$ ($K \neq 0$) is a possible model. It is readily seen that all these models have the same phase (modulo π). A consistent estimator is designed using analytic geometry tools. Its key feature is the characterization of the system frequency behavior (within the set $\{\omega_1, \dots, \omega_m\}$) by a family of static Lissajous curves. Interestingly, the curves correspond precisely to the functions $f(U_k |G(j\omega_k)|x)$ and $f(-U_k |G(j\omega_k)|x)$ and these are nothing other than the nonlinearities associated with the particular models $(G(s)/K, f(Kx))$ and $(-G(s)/K, f(-Kx))$ with $K = U_k |G(j\omega_k)|$. A particularly important fact is that the nonlinearities $f(U_k |G(j\omega_k)|x)$ and $f(-U_k |G(j\omega_k)|x)$ are, less or more, spread versions of $f(x)$ and $f(-x)$, respectively. The couple of models that involve the *less spread* nonlinearity will prove to be the most judicious choice (in regard of gain estimation). One more crucial feature of our solution is that attention is explicitly paid to the *compatibility* between phase estimates and nonlinearity estimate. The above compatibility and spreadability requirements will prove to be essential to guarantee the consistency of the whole identification scheme.

The paper is organized as follows: the identification problem is stated in Section II; geometric characterization of the system frequency behavior is developed in Section III; this characterization is used in Section IV to design the identification scheme; Section V gives complementary analytical expressions; concluding remarks and reference list end the paper.

II. IDENTIFICATION PROBLEM STATEMENT

1) *System Description*: We are considering nonlinear systems that can be described by the Wiener model of Fig. 1 where $G(s)$ denotes the transfer function of the linear subsystem and $f(\cdot)$ is a memoryless nonlinear function. Analytically, the Wiener model is described by the equations

$$x(t) = g(t) * u(t) \quad (1)$$

$$y(t) = w(t) + v(t) \text{ with } w(t) = f(x(t)) \quad (2)$$

where $g(t) = L^{-1}(G(s))$ is the inverse Laplace transform of $G(s)$; the symbol $*$ refers to the convolution operation; $u(t)$ and $y(t)$ are the system input and output, respectively. These are accessible to measurement while the internal signals $x(t)$ and $w(t)$ are not. The equation error $v(t)$ is a random signal that accounts for external noise. It is supposed that:

- i) $G(s)$ is asymptotically stable because system identification is carried out in open loop and;
- ii) for any $T > 0$ and any time-sequence $\{t_k\}$ such that, $t_k - t_{k-1} \geq T$ (for all k), one has: $\{v(t_k)\}$ is a stationary ergodic sequence of zero-mean independent random variables. Ergodicity allows the substitution of arithmetic averages to probabilistic means, making simpler the forthcoming developments.

The frequency domain identification method we are developing necessitates the application of sine signals, $u(t) = U \cos(\omega t)$, for a set of a priori chosen amplitudes

and frequencies $(U, \omega) \in \{(U_k, \omega_k); k = 1, \dots, m\}$. In steady state, the resulting internal signal is

$$x(t) = U |G(j\omega)| \cos(\omega t - \varphi(\omega)) \text{ with } \varphi(\omega) \stackrel{\text{def}}{=} -\angle G(j\omega).$$

With these notations, it is supposed that $f(\cdot)$ is defined on all intervals $-U_k |G(j\omega_k)| \leq x \leq U_k |G(j\omega_k)|$ and falls in the following class of functions:

Assumption A1:

- a) If $f(\cdot)$ is even then, $f(0)$ should be known and $f^{-1}(f(0)) = \{0\}$
- b) If $f(\cdot)$ is not even then, there should exist $-1 \leq \sigma_0 < \sigma_1 \leq 1$ such that $f(\cdot)$ is invertible in the intervals $[\sigma_0 U_k |G(j\omega_k)|, \sigma_1 U_k |G(j\omega_k)|]$ ($k \in \{1, \dots, m\}$), i.e., one has, for all $x \in [\sigma_0 U_k |G(j\omega_k)|, \sigma_1 U_k |G(j\omega_k)|]$ and all $z \in [-U_k |G(j\omega_k)|, U_k |G(j\omega_k)|]$: $f(x) = f(z) \Rightarrow x = z$.

Without loss of generality we suppose that $|G(j\omega_k)| \neq 0$, for all k . Indeed, if $|G(j\omega_k)|$ were zero (for some k) then $x(t)$ would be null and the output $y(t)$ would in turn be null (up to noise). Except for assumption A1, the system is arbitrary. In particular, $G(s)$ and $f(\cdot)$ are not necessarily parametric and the latter is allowed to be nonpolynomial, noninvertible and nonsmooth. Note that Part b of Assumption A1 is not too restrictive because the sizes of the intervals $(\sigma_0 U_k |G(j\omega_k)|, \sigma_1 U_k |G(j\omega_k)|)$ are unknown and may be arbitrarily small (i.e., σ_1 may be too close to σ_0).

2) *Identification Purpose*: We aim at designing an identification scheme that is able to provide a model estimate $(\hat{G}(j\omega), \hat{f}(x))$ representing well the system when this is excited by sinusoidal inputs with the characteristics $(U, \omega) \in \{(U_k, \omega_k); k = 1, \dots, m\}$.

3) *Model Multiplicity*: The complexity of the identification problem mainly comes from the fact that the internal signal $x(t)$ is not accessible for measurement. This in particular implies model multiplicity. Indeed, any couple of the form $(G(s)/K, f(Kx))$ ($K \neq 0$) is a possible model. This naturally leads to the question: what particular model should we focus on? This question will be answered later in Section IV-B. At this point, let us just note that, as long as the phase is concerned, all models are similar to either (G, f) or (G^-, f^-) , depending on the sign of K , where

$$G^-(s) \stackrel{\text{def}}{=} -G(s), \quad f^-(x) \stackrel{\text{def}}{=} f(-x). \quad (3)$$

Therefore, we begin the identification process designing a phase estimator. The main design ingredients are developed in Section III.

III. GEOMETRIC CHARACTERIZATION OF THE SYSTEM FREQUENCY BEHAVIOR

All along this section, the Wiener system is excited by a sine input signal $u(t) = U \cos(\omega t)$ where (U, ω) is any fixed couple belonging to the set $\{(U_k, \omega_k); k = 1, \dots, m\}$. Using the models (G, f) and (G^-, f^-) , the resulting internal signals are respectively defined by the equations

$$x(t) = U |G(j\omega)| \cos(\omega t - \varphi(\omega)) \text{ and } w(t) = f(x(t)) \quad (4a)$$

$$x^-(t) = U |G(j\omega)| \cos(\omega t - \varphi(\omega) - \pi) \text{ and } w(t) = f^-(x^-(t)). \quad (4b)$$

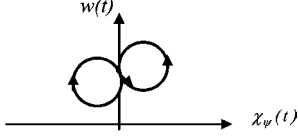


Fig. 2. Example of closed-locus.

A. Characterization of the Curves $(\cos(\omega t - \varphi(\omega)), w(t))$
and $(-\cos(\omega t - \varphi(\omega)), w(t))$

The aim of this subsection is to establish key properties that characterize the parameterized curves $(\cos(\omega t - \varphi(\omega)), w(t))$ and $(-\cos(\omega t - \varphi(\omega)), w(t))$. First, notice that sine signals that oscillate at the same frequency as $\cos(\omega t - \varphi(\omega))$ are of the form:

$$\chi_\psi(t) = \cos(\omega t - \psi) \quad (5a)$$

where $\psi \in \mathbb{R}$ is arbitrary and \mathbb{R} denotes the set of real numbers. It is readily seen that

$$\begin{aligned} \cos(\omega t - \varphi(\omega)) &= \chi_{\varphi(\omega)}(t) \\ -\cos(\omega t - \varphi(\omega)) &= \chi_{\varphi(\omega)+\pi}(t). \end{aligned} \quad (5b)$$

Now, let C_ψ be the parameterized locus constituted of all points of coordinates $(\chi_\psi(t), w(t))$ ($t \geq 0$). As $\chi_\psi(t)$ and $w(t)$ are periodical, with the same period T ($T = 2\pi/\omega$), the curve C_ψ turns out to be an oriented *closed-locus*. Furthermore, C_ψ and $C_{\psi+\pi}$ are *symmetric* with respect to the w -axis, a property that will be useful in the forthcoming development. In general, C_ψ is constituted of one or several loops, (see e.g., Fig. 2). In the particular case where $w(t)$ is a sine signal, C_ψ is a standard Lissajous curve and may present different shapes, e.g., an ellipse, a circle or a line ([18]). The only characteristic of C_ψ that is of interest, for the present study, is its geometric area, denoted $A(\psi)$. Recall that the geometric area of a simple (oriented) loop ignores the loop orientation and, so, is always positive. This is to be distinguished from the algebraic area that may be positive or negative, depending on the loop orientation sense. In the case of a multi-loops locus, the global geometric area equals the sum of the geometric areas of the different single loops. Fig. 2 shows an oriented closed-locus composed of two loops. For the sake of simplicity, these are supposed to be circles of radius r . The geometric area of the whole locus equals $2\pi r^2$ while its algebraic area is null. Now, we are ready to introduce the following definition.

Definition 3.1: The closed-locus C_ψ is said to be static if its geometrical area is null ($A(\psi) = 0$). Then, C_ψ looks like a standard curve (not a closed locus). Inversely, C_ψ is said non-static (or memory) when $A(\psi) \neq 0$.

Proposition 3.1: Consider the Wiener system described by (1)–(2) and Assumption A1, excited by sine inputs $u(t) = U \cos(\omega t)$ with $(U, \omega) \in \{(U_k, \omega_k); k = 1, \dots, m\}$. Then, one has:

- 1) all curves $C_{\varphi(\omega)+h\pi}$ ($h = 0, \pm 1, \pm 2, \dots, \omega = \omega_1, \dots, \omega_m$) are static;
- 2) for any h and any ω , the curve $C_{\varphi(\omega)+2h\pi}$ is symmetric to $C_{\varphi(\omega)+(2h+1)\pi}$ with respect to the ordinate axis (w -axis). \square

Proof:

- 1) From (2), (4) and (5a)–(5b), it follows that:

$$\begin{aligned} w(t) &= f(U |G(j\omega)| \chi_{\varphi(\omega)}(t)) \\ &= f^-(U |G(j\omega)| \chi_{\varphi(\omega)+\pi}(t)). \end{aligned}$$

Since $f(\cdot)$ and $f^-(\cdot)$ are functions (in the standard sense), it follows that $C_{\varphi(\omega)}$ and $C_{\varphi(\omega)+\pi}$ are static curves. The result also holds for $C_{\varphi(\omega)+h\pi}$ (for all h) since

$$\chi_{\varphi(\omega)+h\pi}(t) = \begin{cases} \chi_{\varphi(\omega)}(t) & \text{if } h \text{ is even} \\ \chi_{\varphi(\omega)+\pi}(t) & \text{if } h \text{ is odd.} \end{cases} \quad (6)$$

- 2) Recall that $C_{\varphi(\omega)+h\pi}$ is constituted of the points $(\cos(\omega t - \varphi(\omega)), w(t))$ and $C_{\varphi(\omega)+(2h+1)\pi}$ is the set of points $(-\cos(\omega t - \varphi(\omega)), w(t))$. The above points have the same w -value but opposite abscissas. \blacksquare

Proposition 3.2: Consider the problem statement of Proposition 3.1. If C_ψ is static for some ψ , then one has, for all θ

$$\begin{aligned} f(U |G(j\omega)| \cos(\theta)) &= f(U |G(j\omega)| \cos(\theta - 2(\psi - \varphi(\omega)))) \\ f^-(U |G(j\omega)| \cos(\theta)) &= f^-(U |G(j\omega)| \cos(\theta - 2(\psi - \varphi(\omega)))). \end{aligned}$$

\square

Proof: From (4a)–(4b) one has, for all t

$$\begin{aligned} w(t) &= f(U |G(j\omega)| \cos(\omega t - \varphi(\omega))) \\ &= f^-(U |G(j\omega)| \cos(\omega t - \varphi(\omega))). \end{aligned}$$

On the other hand, if C_ψ is static then there exists a function $g(\cdot)$ such that

$$w(t) = g(\cos(\omega t - \psi)) \quad (7)$$

then, one has for all t

$$\begin{aligned} f(U |G(j\omega)| \cos(\omega t - \varphi(\omega))) &= g(\cos(\omega t - \psi)) \quad (8a) \\ f^-(U |G(j\omega)| \cos(\omega t - \varphi(\omega))) &= g(\cos(\omega t - \psi)). \quad (8b) \end{aligned}$$

Furthermore, it can be easily checked that, for all t

$$\cos\left(\omega\left(t + \frac{\psi}{\omega}\right) - \psi\right) = \cos\left(\omega\left(T - t + \frac{\psi}{\omega}\right) - \psi\right) \quad (9)$$

where $T = 2\pi/\omega$. Then, one gets that, for all t

$$\begin{aligned} g\left(\cos\left(\omega\left(t + \frac{\psi}{\omega}\right) - \psi\right)\right) &= g\left(\cos\left(\omega\left(T - t + \frac{\psi}{\omega}\right) - \psi\right)\right) \end{aligned}$$

which, together with (8a)–(8b), yields (for all t)

$$\begin{aligned} f\left(U |G(j\omega)| \cos\left(\omega\left(t + \frac{\psi}{\omega}\right) - \varphi(\omega)\right)\right) &= f\left(U |G(j\omega)| \cos\left(\omega\left(T - t + \frac{\psi}{\omega}\right) - \varphi(\omega)\right)\right) \\ f^-\left(U |G(j\omega)| \cos\left(\omega\left(t + \frac{\psi}{\omega}\right) - \varphi(\omega)\right)\right) &= f^-\left(U |G(j\omega)| \cos\left(\omega\left(T - t + \frac{\psi}{\omega}\right) - \varphi(\omega)\right)\right) \end{aligned}$$

$$= f^- \left(-U |G(j\omega)| \cos \left(\omega \left(T - t + \frac{\psi}{\omega} \right) - \varphi(\omega) \right) \right).$$

These, respectively, give

$$\begin{aligned} & f(U |G(j\omega)| \cos(\omega t + \psi - \varphi(\omega))) \\ &= f(U |G(j\omega)| \cos(\omega T - \omega t + \psi - \varphi(\omega))) \\ &= f(U |G(j\omega)| \cos(\omega t - \psi + \varphi(\omega))) \\ & f^-(-U |G(j\omega)| \cos(\omega t + \psi - \varphi(\omega))) \\ &= f^-(-U |G(j\omega)| \cos(\omega T - \omega t + \psi - \varphi(\omega))) \\ &= f^-(-U |G(j\omega)| \cos(\omega t - \psi + \varphi(\omega))). \end{aligned}$$

These expressions establish Proposition 3.2 with $\theta = \omega t + \psi - \varphi(\omega)$. As t is arbitrary and the cosine is periodic, the above expressions hold for all θ ■

Proposition 3.3: Consider the problem statement of Proposition 3.1 and suppose that C_ψ is static. Then, one has the following properties:

- 1) if the function $f \cdot$ is not even, then: $\psi - \varphi(\omega) = h\pi$, for some $h = 0, \pm 1, \pm 2, \dots$;
- 2) if the function $f(\cdot)$ is even, then: $\psi - \varphi(\omega) = h\pi$ or $(\pi/2) + h\pi$, for some $h = 0, \pm 1, \pm 2, \dots$

□

Proof: Let us introduce the following notations:

$$\begin{aligned} 2(\psi - \varphi(\omega)) &= \delta(\omega) + 2h\pi & (10) \\ \text{with } 0 \leq \delta(\omega) &< 2\pi \text{ and } h = 0, \pm 1, \pm 2, \dots & (11) \end{aligned}$$

Then, using Proposition 3.2, it follows that, for all $\theta \in [0, 2\pi)$:

$$f(U |G(j\omega)| \cos(\theta)) = f(U |G(j\omega)| \cos(\theta - \delta)). \quad (12)$$

Case 1: $f(\cdot)$ is not even. Using Assumption A1 (Part b), the function f is invertible in the subinterval $(\sigma_0 U |G(j\omega)|, \sigma_1 U |G(j\omega)|)$. Then, from (12) it follows that for any $\theta \in (0, 2\pi)$ such that $\cos(\theta) \in (\sigma_0, \sigma_1)$, one has

$$\cos(\theta) = \cos(\theta - \delta(\omega)). \quad (13)$$

Now, it can easily be checked that if $\delta(\omega) \neq 0$, then for all

$$\begin{aligned} \theta \in (0, 2\pi) - \left\{ \frac{\delta(\omega)}{2}, \pi + \frac{\delta(\omega)}{2} \right\} : \\ \cos(\theta) \neq \cos(\theta - \delta(\omega)). \end{aligned} \quad (14)$$

But this clearly contradicts (13). Hence, $\delta(\omega) = 0$.

Case 2: $f(\cdot)$ is even. Letting $\theta = \pi/2$ in (12), one gets $f(0) = f(U |G(j\omega)| \cos((\pi/2) - \delta(\omega)))$. Then, it follows from Assumption A1 (part a) that $\cos(\pi/2) - \delta(\omega) = 0$, i.e.

$$\delta(\omega) = -2i\pi \text{ or } \delta(\omega) = \pi - 2i\pi \quad (15)$$

for some integer $i = 0, \pm 1, \pm 2, \dots$. This, together with (10) implies that, either $\psi - \varphi = (h - i)\pi$ or $\psi - \varphi = (\pi/2)(h - i)\pi$.

■
Proposition 3.4: Consider the problem statement of Proposition 3.1. If C_ψ is static then there is a unique function $g(\cdot)$, such that: $g(\cos(\omega t - \psi)) = w(t), \forall t$. More specifically, for all $z \in [-1, +1]$

$$g(z) = \begin{cases} f(U |G(j\omega)| z) & \text{if } \psi - \varphi(\omega) = 2h\pi \\ f^- (U |G(j\omega)| z) & \text{if } \psi - \varphi(\omega) = \pi + 2h\pi \end{cases}$$

for some integer h □

Proof: The fact that C_ψ is static guarantees the existence of a $g(\cdot)$ such that

$$g(\cos(\omega t - \psi)) = w(t), \quad \forall t. \quad (16)$$

The uniqueness of $g(\cdot)$ is now proved separating the two cases pointed out in Assumption A1.

Case 1: the function $f(\cdot)$ is not even. Using Proposition 3.3 (part 1) it follows that $\psi - \varphi(\omega) = h\pi$, for some $h = 0, \pm 1, \pm 2, \dots$. Then (16), implies

$$g((-1)^h \cos(\omega t - \varphi(\omega))) = w(t), \quad \forall t. \quad (17)$$

Comparing (17) with (4a) yields

$$g((-1)^h \cos(\omega t - \varphi(\omega))) = f(U |G(j\omega)| \cos(\omega t - \varphi(\omega)))$$

which implies that, for all $\forall z \in [-1, +1]$

$$g(z) = f(U |G(j\omega)| z) \text{ if } h \text{ is even} \quad (18)$$

$$g(z) = f^- (U |G(j\omega)| z) \text{ if } h \text{ is odd.} \quad (19)$$

Hence, Proposition 3.4 holds in Case 1.

Case 2: $f(\cdot)$ is even. Using Proposition 3.3 (Part 2), it follows that:

$$\psi - \varphi(\omega) = k\pi \text{ or } \psi - \varphi(\omega) = \frac{\pi}{2} + k\pi \quad (20)$$

for some $h = 0, \pm 1, \pm 2, \dots$. Let us show, by contradiction, that the second solution in (20) can not hold. Assume that, for some integer k

$$\psi - \varphi(\omega) = \frac{\pi}{2} + k\pi. \quad (21)$$

It follows from (16) that:

$$g((-1)^k \sin(\omega t - \varphi(\omega))) = w(t), \quad \forall t. \quad (22)$$

Again, comparing (22) and (4a), one gets

$$g((-1)^k \sin(\omega t - \varphi(\omega))) = f(U |G(j\omega)| \cos(\omega t - \varphi(\omega))).$$

This can be rewritten in a more compact form, letting

$$g((-1)^k \sin(\theta)) = f(U |G(j\omega)| \cos(\theta)), \quad (\text{for all } \theta). \quad (23)$$

Substituting $\theta + \pi$ to θ in (23) implies that, for all θ

$$g\left(-(-1)^k \sin(\theta)\right) = f(-U |G(j\omega)| \cos(\theta)). \quad (24)$$

As f is even, it follows, comparing (23)–(24), that g , in turn, is even. Then, one gets from (23) that:

$$f(U|G(j\omega)|\cos(\theta)) = g\left(\sqrt{1-\cos^2(\theta)}\right) \quad (\text{for all } \theta). \quad (25)$$

Using the variable change $z = \sqrt{1-\cos^2(\theta)}$, it follows from (25) that, $\forall z \in [-1, +1]$:

$$g(z) = f\left(U|G(j\omega)|\sqrt{1-z^2}\right). \quad (26)$$

Let us check that such a solution $g(\cdot)$ is not admissible in the sense of Assumption A1 (part a). Indeed, one readily gets from (26) that

$$g(0) = f(U|G(j\omega)|). \quad (27)$$

On the other hand, it follows from Assumption A1 (part a) that:

$$f(x) = f(0) \Rightarrow x = 0. \quad (28)$$

Since $|G(j\omega)| \neq 0$ (for all $\omega \in \{\omega_1, \dots, \omega_m\}$) it follows from (27)–(28) that $g(0) \neq f(0)$. This clearly shows that $g(\cdot)$ does not satisfy assumption A1 (part a) and, so, is not admissible. Hence, the solution (21) must be discarded. Then, in view of (20), one necessarily has: $\psi - \varphi = k\pi$. The rest of the proof is similar to Case 1. Proposition 3.4 is established ■

B. Estimation of the Parameterized Curves

Propositions 3.3 and 3.4 are quite interesting. The first shows that $\varphi(\omega) = -\angle G(j\omega)$ can be recovered (modulo π) by just tuning the parameter ψ until the closed-locus C_ψ becomes static. Due to Proposition 3.4, the obtained static curve is precisely the graphical plot of either $f(U|G(j\omega)|x)$ or $f(-U|G(j\omega)|x)$. Now, the main issue is that the locus C_ψ depends on the signal $w(t)$ which is not accessible for measurement. This is presently coped with making full use of the information at hand, namely the periodicity (with period $2\pi/\omega$) of both $X_\psi(t)$ and $w(t)$ and the ergodicity of the noise $w(t)$. Bearing these in mind, the relation $y(t) = w(t) + v(t)$ suggests the following estimator:

$$\hat{w}(t, N) \stackrel{\text{def}}{=} \frac{1}{N} \sum_{k=1}^N y(t+kT); \quad t \in [0, T] \quad (29)$$

where $T = 2\pi/\omega$ and N is a sufficiently large integer. Specifically, for a fixed time instant t , the quantity $\hat{w}(t, N)$ is the mean value of the (measured) sequence $\{y(t+kT); k = 0, 1, 2, \dots\}$. Then, an estimate $\hat{C}_{\psi, N}$ of C_ψ is simply obtained substituting $\hat{w}(t, N)$ to $w(t)$ when constructing C_ψ . Accordingly, $\hat{C}_{\psi, N}$ turns out to be the parameterized locus including all points $(\chi_\psi(t), \hat{w}(t, N))$ ($t \geq 0$). These remarks lead to the following proposition:

Proposition 3.5: Consider the problem statement of Proposition 3.1. Then, one has:

- 1) $\hat{w}(t, N)$ converges in probability to $w(t)$ (as $N \rightarrow \infty$).
- 2) $\hat{C}_{\psi, N}$ converges in probability to C_ψ (as $N \rightarrow \infty$) i.e., for all $t \geq 0$

$$\lim_{N \rightarrow \infty} (\chi_\psi(t), \hat{w}(t, N)) = (\chi_\psi(t), w(t)) \quad (\text{w.p.1}). \quad (30)$$

- 3) Consequently, if $\psi = \varphi(\omega) + h\pi$ then $\lim_{N \rightarrow \infty} \hat{C}_{\psi, N}$ is static (w.p.1).
- 4) Inversely, if $\lim_{N \rightarrow \infty} \hat{C}_{\psi, N}$ is static for some ψ , then one of the following statements hold w.p.1:
 - a) $\psi = \varphi(\omega) + 2h\pi$ (for some $h = 0, \pm 1, \pm 2, \pm 3, \dots$) and the mapping $\cos(\omega t - \psi) \rightarrow \hat{w}(t, N)$ coincides with the curve of the function $f(U|G(j\omega)|x)$ for $x \in [-1, +1]$.
 - b) $\psi = \varphi(\omega) + \pi + 2h\pi$ (for some $h = 0, \pm 1, \pm 2, \pm 3, \dots$) and the mapping $\cos(\omega t - \psi) \rightarrow \hat{w}(t, N)$ coincides with the curve of $f^-(U|G(j\omega)|x)$ for $x \in [-1, +1]$.

□

Proof: From (2) one gets that, for all $t \in [0, T]$

$$y(t) = w(t) + v(t). \quad (31)$$

Then, using the fact that $w(t)$ is periodic with period T , it follows from (31) that, for all $t \in [0, T]$ and all integers k : $y(t+kT) = w(t) + v(t+kT)$, which in turn implies that:

$$\hat{w}(t, N) = \frac{1}{N} \sum_{k=1}^N y(t+kT) = w(t) + \frac{1}{N} \sum_{k=1}^N v(t+kT). \quad (32)$$

Since $\{v(t_k)\}$, with $t_k = t+kT$, is zero mean and ergodic, the last term on the right side vanishes w.p.1 as $N \rightarrow \infty$. This proves Part 1 of the proposition. To prove Part 2, notice that, using the fact that both $\chi_\psi(t)$ and $w(t)$ are periodic (with period T), one has:

$$(x_\psi(t+kT), y(t+kT)) = (x_\psi(t), w(t)) + (0, v(t+kT)).$$

Averaging both sides (with respect to k) gives

$$\left(x_\psi(t), \frac{1}{N} \sum_{k=1}^N y(t+kT) \right) = (x_\psi(t), w(t)) + \left(0, \frac{1}{N} \sum_{k=1}^N v(t+kT) \right). \quad (33)$$

Again, the last term on the right side vanishes w.p.1 as $N \rightarrow \infty$, for the same reasons as above. This proves Part 2 of the proposition. Part 3 is a consequence of Part 2 and Proposition 3.1. Part 4 follows from Part 2 using Proposition 3.4 ■

Remark 3.1: In the light of Proposition 3.5 (Part 4) it is seen that, for sufficiently large N , all curves belonging to the family $\{\hat{C}_{\varphi(\omega_k), N}; k = 1, \dots, m\}$ are static and any one of them is a, more or less, spread version of all the others. The same remark applies to the family $\{\hat{C}_{\varphi(\omega_k)+\pi, N}; k = 1, \dots, m\}$.

IV. FREQUENCY IDENTIFICATION METHOD FOR WIENER SYSTEMS

A. Graphical Phase Estimation (GPE)

Proposition 3.5 and Remark 3.1 suggest the following phase estimator:

GPE1. Apply the input signal $u(t) = U \cos(\omega t)$ to the nonlinear system of interest for $(U, \omega) \in \{(U_1, \omega_1), \dots, (U_m, \omega_m)\}$.

GPE2. Get a recording of the output $y(t)$ over a sufficiently large interval of time $0 \leq t \leq NT$. Generate the continuous signals $\hat{w}(t, N-1)$ and $\hat{w}(t, N)$ using (29). Compute the $L_2[0, T]$ norms, i.e., $\|\hat{w}(N)\|_2 = \left(\int_0^T \hat{w}(t, N)^2 dt\right)^{1/2}$ and $\|\hat{w}(N) - \hat{w}(N-1)\|_2 = \left(\int_0^T (\hat{w}(t, N) - \hat{w}(t, N-1))^2 dt\right)^{1/2}$. Choose a threshold $0 < \varepsilon \ll 1$. If $(\|\hat{w}(N) - \hat{w}(N-1)\|_2 / \|\hat{w}(N)\|_2) < \varepsilon$ then go to Step GPE3. Otherwise, increase the value of N and repeat Step GPE2 starting from the beginning.

GPE3. Plot the (closed) parameterized curve $\hat{C}_{\psi, N} = \{(\cos(\omega t - \psi), \hat{w}(t, N)), 0 \leq t \leq NT\}$, for different values of ψ until a static curve is observed. Let ψ^* denote the first value of ψ such that $C_{\psi, N}$ is static. Then, $\hat{\phi}_N(\omega) = \psi^*$ is the estimate of either $\varphi(\omega)$ or $\varphi(\omega) + \pi$.

GPE4. Repeat the above steps for all $(U, \omega) \in \{(U_1, \omega_1), \dots, (U_m, \omega_m)\}$. Check that each curve is a, more or less, spread version of the others. If, for some ω , one gets a curve that is not coherent with those obtained previously, then take $\hat{\phi}_N(\omega) = \psi^* + \pi$ where ψ^* is as in GPE3.

It is worth noting that the correction (by π) in the step GPE4 ensures that the phase estimator $\hat{\phi}_N(\omega)$ focuses either on $\varphi(\omega) = -\angle G(j\omega)$ (for all $\omega \in \{\omega_1, \dots, \omega_m\}$) or on $\varphi(\omega) + \pi$ (for all ω). In fact, it does not matter to know which one is being focused on. The main point is that the estimator focuses either on $G(s)$ or on $G^-(s)$ (but not on both). This remark together with the results of Proposition 3.5 guarantee the consistency of the estimator $\hat{\phi}_N(\omega)$. This is formalized in the following theorem:

Theorem 4.1: Consider the problem statement of Proposition 3.1. The phase estimator $\hat{\phi}_N(\omega)$, defined by the procedure GPE1-GPE4, is consistent in the sense that one has w.p.1, either $\lim_{N \rightarrow \infty} \hat{\phi}_N(\omega) = \varphi(\omega)$ (for all ω) or $\lim_{N \rightarrow \infty} \hat{\phi}_N(\omega) = \varphi(\omega) + \pi$ (for all ω). \square

B. Graphical Nonlinearity Estimation (NLE)

Let us consider the family of (static) curves $\hat{\Gamma}_{\omega, N} \stackrel{def}{=} \hat{C}_{\hat{\phi}_N(\omega), N}$ constructed in the phase estimation procedure GPE1-GPE4. In the light of Proposition 3.5 and Theorem 4.1, it is clear that, for any fixed couple $(U, \omega) \in \{(U_1, \omega_1), \dots, (U_m, \omega_m)\}$, the curve $\hat{\Gamma}_{\omega, N}$ converges in probability to (the graphical plot of) either $f(U|G(j\omega)|x)$ or $f^-(U|G(j\omega)|x)$ (where $-1 \leq x \leq 1$). Therefore, a consistent estimate of either $f(U_k|G(j\omega_k)|x)$ or $f^-(U_k|G(j\omega_k)|x)$ can be recovered from the curve $\hat{\Gamma}_{\omega_k, N}$ ($k = 1, \dots, m$). The question is: what use can be made of an estimate of $f(U_k|G(j\omega_k)|x)$ or $f^-(U_k|G(j\omega_k)|x)$?

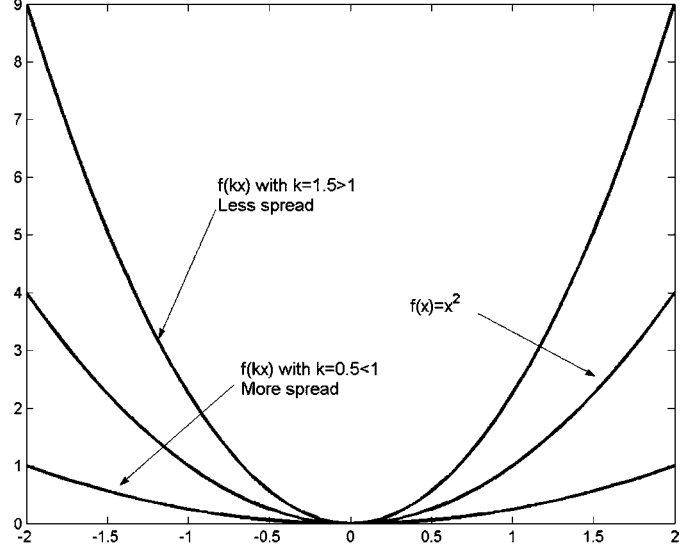


Fig. 3. Example of a nonlinearity and its spread versions.

This question is answered exploiting model multiplicity pointed out in Section II. Specifically, the above functions are nothing other than the nonlinearities of the particular couple of models

$$M(U_k, \omega_k) \stackrel{def}{=} \left(\frac{G(s)}{U_k |G(j\omega_k)|}, f(U_k |G(j\omega_k)|x) \right)$$

$$M^-(U_k, \omega_k) \stackrel{def}{=} \left(\frac{G^-(s)}{U_k |G(j\omega_k)|}, f^-(U_k |G(j\omega_k)|x) \right)$$

respectively. That is, for any $k \in \{1, \dots, m\}$, the curve $\hat{\Gamma}_{\omega_k, N}$ converges (in probability) to the nonlinearity of either $M(U_k, \omega_k)$ or $M^-(U_k, \omega_k)$ (it does not matter to know which one). Then, it makes sense to limit the identification to the model family $\{M(U_k, \omega_k), M^-(U_k, \omega_k); k = 1, \dots, m\}$. But, what particular model of this family should one focus on?

To answer such a question, notice that the functions $f(U_k |G(j\omega_k)|x)$ and $f(-U_k |G(j\omega_k)|x)$ are more or less spread versions of $f(x)$ and $f(-x)$, respectively. Specifically, $f(U_k |G(j\omega_k)|x)$ is more spread than $f(x)$ if $U_k |G(j\omega_k)| < 1$. Otherwise, $f(U_k |G(j\omega_k)|x)$ is less spread than (and so it is a concentrated version of) $f(x)$. The same remark applies to $f(-U_k |G(j\omega_k)|x)$ compared to $f(-x)$. As the functions of interest, namely $f(U_k |G(j\omega_k)|x)$ and $f(-U_k |G(j\omega_k)|x)$, are all defined in the same interval, i.e., $-1 \leq x \leq 1$, it is judicious to focus on the couple of models that involve the less spread (or, equivalently, the most concentrated) nonlinearity (see Fig. 3).

Let $(M(\bar{U}, \bar{\omega}), M^-(\bar{U}, \bar{\omega}))$ denote such couple where $(\bar{U}, \bar{\omega}) \in \{(U_1, \omega_1), \dots, (U_m, \omega_m)\}$. For convenience, the corresponding elements are, respectively, denoted $(\bar{G}(s), \bar{f}(x))$ and $(\bar{G}^-(s), \bar{f}^-(x))$, i.e.

$$\bar{G}(s) \stackrel{def}{=} \frac{1}{\bar{U} |G(j\bar{\omega})|} G(s) \quad \bar{G}^-(s) \stackrel{def}{=} -\bar{G}(s) \quad (34)$$

$$\bar{f}(x) \stackrel{def}{=} f(\bar{U} |G(j\bar{\omega})|x), \quad \bar{f}^-(x) \stackrel{def}{=} \bar{f}(-x) \quad (35)$$

where $x \in [-1, +1]$. Focusing on $(M(\bar{U}, \bar{\omega}), M^-(\bar{U}, \bar{\omega}))$ will prove to be the most convenient choice when it comes to estimating the gains $|\bar{G}(j\omega)|$ ($\omega \in \{\omega_1, \dots, \omega_m\}$).

On the other hand, as $f(\bar{U} |G(j\bar{\omega})| x)$ is the less spread function in the family $\{f(U_k |G(j\omega_k)| x), k = 1, \dots, m\}$, one necessarily has

$$U_k |G(j\omega_k)| \leq \bar{U} |G(j\bar{\omega})| \quad (k = 1, \dots, m). \quad (36)$$

Finally, recall that $\angle \bar{G}(j\omega) = \angle G(j\omega)$ and $\angle \bar{G}^-(j\omega) = \angle G^-(j\omega)$, for all ω . That is, the estimator defined by GPE1-GP4, is still convenient in the sense that $\hat{\phi}_N(\omega)$ converges in probability to $\bar{\varphi}(\omega) \stackrel{def}{=} -\angle \bar{G}(j\omega)$ for all $\omega \in \{\omega_1, \dots, \omega_m\}$ or it converges to $\bar{\varphi}(\omega) + \pi$, for all ω . Taking these remarks into account, we propose the following algorithm to get a nonlinearity estimate $\hat{f}_N(\cdot)$:

NLE1 . Consider the family of static curves $\hat{\Gamma}_{\omega, N} \stackrel{def}{=} \hat{C}_{\hat{\phi}_N(\omega), N}$, constructed in the phase estimation procedure GPE1-GPE4. Select the most concentrated (i.e., less spread) curve and let $\bar{\omega}$ denote the corresponding frequency.

NLE2 . Let $g(x)$ (with $x \in [-1, +1]$) be the function induced by the static curve $\hat{\Gamma}_{\bar{\omega}, N}$.

NLE3 . If $g(\cdot)$ is not even, then take $\hat{f}_N = g$.

NLE4 . If $g(\cdot)$ is even, conclude that (within $[-1, +1]$)

$$\hat{f}_N(x) = \begin{cases} g(x) & \text{if } g(0) = f(0) \\ g(\sqrt{1-x^2}) & \text{otherwise.} \end{cases}$$

Remark 4.1: The fact that $f(0)$ is known (Assumption A1, part a) has been used in Step NLE4. The estimate \hat{f}_N thus obtained may correspond to either \bar{f} or \bar{f}^- , depending on the phase estimate $\hat{\phi}_N(\bar{\omega})$. This is made precise in the following theorem which is a direct consequence of Proposition 3.5 and Theorem 4.1.

Theorem 4.2: Consider the problem statement of Proposition 3.1. The nonlinearity estimator NLE1-NLE4, is consistent in the sense that one has w.p.1:

- if $\lim_{N \rightarrow \infty} \hat{\phi}_N(\bar{\omega}) = \varphi(\bar{\omega})$ then $\lim_{N \rightarrow \infty} \hat{f}_N(x) = \bar{f}(x)$, for all $\forall x \in [-1, +1]$;
- if $\lim_{N \rightarrow \infty} \hat{\phi}_N(\bar{\omega}) = \varphi(\bar{\omega}) + \pi$ then $\lim_{N \rightarrow \infty} \hat{f}_N(x) = \bar{f}^-(x)$, for all $\forall x \in [-1, +1]$.

□

Remarks 4.2:

- In the case where this may be of interest, a polynomial representation can, afterward, be given to the nonlinearity $\hat{f}_N(x)$ interpolating a number of points selected on the curve $\hat{\Gamma}_{\bar{\omega}, N}$.
- In [1], model rescaling (34)–(35) has also been used to cope with the estimation of the nonlinearity. However, it was suggested there that $\bar{\omega}$ may be chosen arbitrary. Doing so, the gains $|\bar{G}(j\omega_k)|$ can not be consistently estimated as explained in Section IV-C.

C. Gain Modulus Estimation

The phase estimates $\hat{\phi}_N(\omega_k)$ ($k = 1, \dots, m$) and the nonlinearity estimate \hat{f}_N obtained previously will now be used to get estimates $|\hat{G}(j\omega_k)|$ of the gains $|\bar{G}(j\omega_k)|$ ($k \in \{1, \dots, m\}$). To keep simple the forthcoming presentation, it is temporarily

assumed that $\hat{f}_N = \bar{f}$, $\hat{\phi}_N(\omega_k) = \bar{\varphi}(\omega_k) = -\angle \bar{G}(j\omega_k)$ (for all $k \in \{1, \dots, m\}$) and $v(t) = 0$ (no noise). In the procedure GPE1-GPE3, the Wiener system has been excited by the family of signals $u(t) = U_k \cos(\omega_k t)$ ($k = 1, \dots, m$). Using the model $(\bar{G}(s), \bar{f}(x))$, the Wiener system signals can be expressed as follows:

$$y(t) = w(t) = \bar{f}(|\bar{G}(j\omega_k)| U_k \cos(\omega_k t - \bar{\varphi}(\omega_k))) \quad (37)$$

with $\bar{\varphi}(\omega_k) = -\angle \bar{G}(j\omega_k)$. On the other hand, it readily follows from (34) and (36) that:

$$U_k |\bar{G}(j\omega_k)| \leq 1 \quad (k = 1, \dots, m). \quad (38)$$

If \bar{f} were invertible, then the internal signal $x(t) = \bar{f}^{-1}(y(t)) = |\bar{G}(j\omega_k)| U_k \cos(\omega_k t - \bar{\varphi}(\omega_k))$ would be available and, so, $|\bar{G}(j\omega_k)|$ would be easily recovered. The situation becomes much more problematic when \bar{f} is not invertible. Nevertheless, the gains $|\bar{G}(j\omega_k)|$ can still be uniquely determined if the system nonlinearity satisfies, in addition to Assumption A1, the following assumption:

Assumption A2: If f is even then, there exist $0 \leq \sigma'_0 < \sigma'_1 \leq 1$ such that, for all $k \in \{1, \dots, m\}$, all $x \in [\sigma'_0 U_k |G(j\omega_k)|, \sigma'_1 U_k |G(j\omega_k)|]$ and all $z \in [0, U_k |G(j\omega_k)|]$, one has: $f(x) = f(z) \Rightarrow x = z$.

Remark 4.3: Let f be any function satisfying Assumptions A1–A2. The following properties hold:

- If f is even then it is invertible at $x = 0$ and $f(0)$ is known (Assumption A1, Part a). Furthermore, one gets from Assumption A2 that, for all k , the branch of f corresponding to the (unilateral) interval $[0, U_k |G(j\omega_k)|]$ is locally invertible on the subintervals $x \in [\sigma'_0 U_k |G(j\omega_k)|, \sigma'_1 U_k |G(j\omega_k)|]$. For instance, the function $f(x) = x^2$ satisfies both Assumptions A1 (Part a) and A2, the numbers (σ'_0, σ'_1) are then arbitrary.
- It has already been noticed that \bar{f} is a less or more spread version of f . Therefore, \bar{f} also satisfies Assumptions A1–A2. More precisely,
 - in the case where \bar{f} is even, replace in Assumption A2, the intervals $[-U_k |G(j\omega_k)|, U_k |G(j\omega_k)|]$ and $[0, U_k |G(j\omega_k)|]$ by $[-U_k |\bar{G}(j\omega_k)|, U_k |\bar{G}(j\omega_k)|]$ and $[0, U_k |\bar{G}(j\omega_k)|]$, respectively;
 - in the case where \bar{f} is not even, replace in Assumption A1 (Part b) the intervals $[-U_k |G(j\omega_k)|, U_k |G(j\omega_k)|]$ and $[\sigma_0 U_k |G(j\omega_k)|, \sigma_1 U_k |G(j\omega_k)|]$ by $[-U_k |\bar{G}(j\omega_k)|, U_k |\bar{G}(j\omega_k)|]$ and $[\sigma_0 U_k |\bar{G}(j\omega_k)|, \sigma_1 U_k |\bar{G}(j\omega_k)|]$, respectively.

Now, it will be shown that, under Assumptions A1–A2, the gain $|\bar{G}(j\omega_k)|$ ($k \in \{1, \dots, m\}$) can exactly be estimated using the following algorithm, where $k \in 1, \dots, m$:

$$|\hat{G}(j\omega_k)| = \arg \min_{0 \leq \alpha \leq (1/U_k)} J_k(\alpha) \quad (39a)$$

$$J_k(\alpha) \stackrel{def}{=} \int_{t=0}^T [w(t) - \bar{f}(\alpha U_k \cos(\omega_k t - \bar{\varphi}(\omega_k)))]^2 dt. \quad (39b)$$

Proposition 4.1: Consider the optimization problem defined by (39a)–(39b) in presence of the constraint (37), where \bar{f} satisfies Assumptions A1–A2 (as this is made precise in Remark 4.3

(part 2)). Then, for all k , $J_k(\alpha)$ has a unique global minimum at $|\hat{G}(j\omega_k)| = |\overline{G}(j\omega_k)|$ \square

Proof: It is readily seen from (39b) that $J_k(|\overline{G}(j\omega_k)|) = 0$, which means that $|\overline{G}(j\omega_k)|$ is a global minimum. Let us show that such a minimum is unique. To this end, let α denotes any real such that $J_k(\alpha) = 0$. It follows from (37) and (39b) that, for almost all $t \in [0, T]$:

$$\begin{aligned} & \overline{f}(|\overline{G}(j\omega_k)| U_k \cos(\omega_k t - \overline{\varphi}(\omega_k))) \\ &= \overline{f}(\alpha U_k \cos(\omega_k t - \overline{\varphi}(\omega_k))). \end{aligned} \quad (40)$$

On the other hand, it is obvious that for all $t \in [0, T]$ such that $\sigma_0 < \cos(\omega_k t - \overline{\varphi}(\omega_k)) < \sigma_1$, one has

$$\begin{aligned} \sigma_0 U_k |\overline{G}(j\omega_k)| &< |\overline{G}(j\omega_k)| U_k \cos(\omega_k t - \overline{\varphi}(\omega_k)) \\ &< \sigma_1 U_k |\overline{G}(j\omega_k)|. \end{aligned} \quad (41a)$$

Similarly, for all $t \in [0, T]$ such that $\sigma'_0 \cos(\omega_k t - \overline{\varphi}(\omega_k)) < \sigma'_1$, one has

$$\begin{aligned} \sigma'_0 U_k |\overline{G}(j\omega_k)| &< |\overline{G}(j\omega_k)| U_k \cos(\omega_k t - \overline{\varphi}(\omega_k)) \\ &< \sigma'_1 U_k |\overline{G}(j\omega_k)|. \end{aligned} \quad (41b)$$

Now, let us distinguish between the two cases pointed out in Assumptions A1–A2.

Case 1: \overline{f} is even. Using Assumptions A1 (Part a) and A2 and Remark 4.3 (part 2), it follows from (40) that: $|\overline{G}(j\omega_k)| U_k \cos(\omega_k t - \overline{\varphi}(\omega_k)) = \alpha U_k \cos(\omega_k t - \overline{\varphi}(\omega_k))$, for all t such that (41b) holds. This readily gives $\alpha = |\overline{G}(j\omega_k)|$.

Case 2: \overline{f} is not even. Using Assumption A1 (part b) and Remark 4.3 (part 2), it follows from (40) that $|\overline{G}(j\omega_k)| U_k \cos(\omega_k t - \overline{\varphi}(\omega_k)) = \alpha U_k \cos(\omega_k t - \overline{\varphi}(\omega_k))$, for all t such that (41a) holds. This implies that $\alpha = |\overline{G}(j\omega_k)|$.

Hence, uniqueness of the global minimum of $J_k(\cdot)$ is proved in all cases \blacksquare

Remark 4.4:

- 1) A crucial feature that makes the optimization problem (39a)–(39b) well posed is that the function \overline{f} is defined for all possible values of its argument, i.e., $|\overline{G}(j\omega_k)| U_k \cos(\omega_k t - \overline{\varphi}(\omega_k))$ with $t \in [0, T]$ and $k = 1, \dots, m$. Indeed, (38) ensures that the above argument belongs to $[-1, 1]$, which is an interval of definition of \overline{f} . Accordingly, the minimum search in (39a) is limited to the interval $0 \leq \alpha \leq (1/U_k)$.
- 2) It is important to note that the above well posedness (of the optimization problem (39a-b)) is a direct consequence of our choice to focus on the particular models $(\overline{G}(s), \overline{f}(x))$ and $(\overline{G}^-(s), \overline{f}^-(x))$ that involve the functions $\overline{f}(x) \stackrel{def}{=} f(\overline{U}|G(j\overline{\omega})|x)$ and $\overline{f}^-(x) \stackrel{def}{=} f(-\overline{U}|G(j\overline{\omega})|x)$ which are most concentrated (less spread) on $[-1, 1]$ [see (34)–(36)].
- 3) While the proposed optimization-based approach is largely inspired from [1], it is worth noting that the spread requirement (applied when selecting the models $(\overline{G}, \overline{f})$ and $(\overline{G}^-, \overline{f}^-)$) is entirely new. Indeed, it is suggested in

[1] that the function (here denoted \overline{f}) involved in (39b), can be arbitrarily chosen (see Assumption A3.1 in that paper and subsequent comments). If we did so, there would be no guarantee that all arguments of interest, i.e., $|\overline{G}(j\omega_k)| U_k \cos(\omega_k t - \overline{\varphi}(\omega_k))$, belong to the definition interval $[-1, 1]$. Then, the minimum search interval in (39a-b) may not include the global minimum, $|\overline{G}(j\omega_k)|$, for some values of k .

Proposition 4.1 is now used to build up a consistent estimator of the gains $|\overline{G}(j\omega_k)|$ in presence of not necessarily null noise $v(t)$. Then, (37) becomes

$$y(t) = w(t) + v(t) \quad (42a)$$

$$w(t) = \overline{f}(|\overline{G}(j\omega_k)| U_k \cos(\omega_k t - \overline{\varphi}(\omega_k))). \quad (42b)$$

Given the estimates \hat{f}_N and $\hat{\varphi}_N(\omega_k)$ ($k \in \{1, \dots, m\}$), of the nonlinearity and phase, Algorithm (39a-b) suggests the following gain estimator:

$$\begin{aligned} & |\hat{G}_N(j\omega_k)| \\ &= \arg \min_{0 \leq \alpha \leq (1/U_k)} J_{k,N}(\alpha) \end{aligned} \quad (43a)$$

$$\begin{aligned} & J_{k,N}(\alpha) \\ &\stackrel{def}{=} \int_{t=0}^T \left[\hat{w}(t, N) - \hat{f}_N \left(\alpha U_k \cos \left(\omega_k t - \hat{\varphi}_N(\omega_k) \right) \right) \right]^2 dt \end{aligned} \quad (43b)$$

where $\hat{w}(t, N)$ is defined by (29), i.e.

$$\hat{w}(t, N) \stackrel{def}{=} \frac{1}{N} \sum_{k=1}^N y_k(t + kT). \quad (43c)$$

Theorem 4.3: Consider the Wiener system described by (1)–(2) and suppose that the involved nonlinearity satisfies Assumptions A1-A2. Let the system be excited by the same input signals as in procedure GPE1-GPE4, i.e., $u(t) = U_k \cos(\omega_k t)$ ($k = 1, \dots, m$). The system can also be modelled by $(\overline{G}, \overline{f})$, defined by (34)–(35), and the nonlinearity \overline{f} in turn satisfies Assumptions A1-A2 [as this is made precise in Remark 4.3 (part 2)]. Then, the gain estimator (43a)–(43c) is consistent i.e., $|\hat{G}_N(j\omega_k)|$ converges in probability to $|\overline{G}(j\omega_k)|$, as $N \rightarrow \infty$. \square

Proof: In view of Proposition 4.1, it is sufficient to show that $J_{k,N}(\alpha)$ converges in probability to $J_k(\alpha)$ as $N \rightarrow \infty$. To this end, note that, by Proposition 3.5 (Part 1), $\hat{w}(t, N)$ converges in probability to $w(t)$, for all $t \in [0, T]$, (as $N \rightarrow \infty$). Furthermore, it was shown in Theorems 4.1 and 4.2 that one of the following statements holds w.p.1, as $N \rightarrow \infty$:

- i) $\hat{\varphi}_N(\omega_k)$ converges to $\overline{\varphi}(\omega_k) \stackrel{def}{=} -\angle \overline{G}(j\omega_k)$ (for all k) and \hat{f}_N converges to \overline{f} .
- ii) $\hat{\varphi}_N(\omega_k)$ converges to $\overline{\varphi}(\omega_k) + \pi$ (for all k) and \hat{f}_N converges to \overline{f}^- .

In the light of these remarks, it is readily seen comparing (39b) and (43b) that $J_{k,N}(\alpha)$ actually converges in probability to $J_k(\alpha)$ as $N \rightarrow \infty$ \blacksquare

Remark 4.5:

- 1) Since (43b) has a unique minimum, this can be found graphically plotting $J_N(\alpha)$ against $\alpha \in [0, 1/U_k]$.

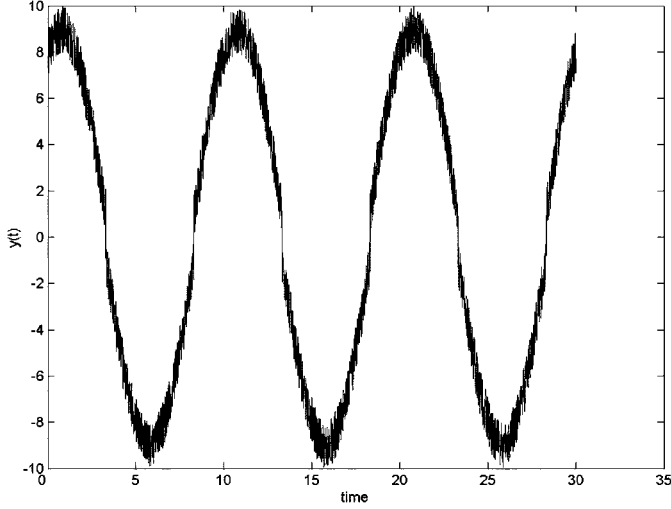


Fig. 4. Output $y(t)$ obtained over three periods with $\omega = \omega_1 = 0.2\pi$ rad/s (simulation of Section IV-D-I).

- 2) The gain estimator in [1] was only considered in the absence of noise and, even in this case, no formal convergence analysis has been given. The absence of formal analysis in that paper can be explained by the shortcoming pointed out in Remark 4.4 (part 3).

D. Simulation Results

1) *Identification in Presence of Discontinuous Nonlinearity:* The graphical identification method described previously is now illustrated considering a Wiener system characterized by

$$G(s) = \frac{4(1 - \frac{s}{\pi})}{(1 + \frac{s}{\pi})(1 + \frac{0.5s}{\pi})} \quad (44a)$$

$$f(x) = \text{sign}(x)(\text{abs}(x) + 1). \quad (44b)$$

Note that $G(s)$ involves a large phase variation, due to its nonminimum phase feature. The nonlinearity $f(\cdot)$ is a preload with an abrupt discontinuity at $x = 0$. According to the proposed identification method, the system is excited by 6 sinusoids of the form $u(t) = U_k \cos(\omega_k t)$ ($k = 1, \dots, 6$), where the couples (U_k, ω_k) are given the values of Table I. The output is disturbed by a zero-mean noise $v(t)$ randomly uniformly distributed in $[-1, +1]$. Fig. 4 shows the (steady state) output signal, $y(t)$, obtained with $\omega = \omega_1 = 0.2\pi$ rad. The phase estimator GPE1-GPE4 is first applied to get phase estimates $\hat{\phi}_N(\omega_k)$. The way in which the estimator operates is illustrated here for $\omega_1 = 0.2\pi$ rad/s. First, the average output $\hat{w}(t, N)$ is generated according to (29) (with $N = 30$) and used to construct the parameterized closed-locus $\hat{C}_{\psi, N} = \{(\cos(\omega_1 t - \psi), \hat{w}(t, N)); 0 \leq t \leq NT\}$ ($T = 2\pi/\omega_1$) for different values of ψ . The curves corresponding to four values of ψ are shown by Fig. 5. It is seen that a static curve is obtained for $\psi^* = 0.49$ rad. Then, it is concluded that $\hat{\phi}_N(\omega_1) = \psi^* = 0.49$ rad which, in fact, is nothing other than $\varphi(\omega_1) = -\angle G(j\omega_1)$. The phase estimates $\hat{\phi}_N(\omega_k)$ obtained for the different frequencies ω_k ($k = 1, \dots, 6$) are given by Table I. Notice that they all correspond to $\varphi(\omega_k) = -\angle G(j\omega_k)$.

The static curves $\hat{\Gamma}_{\omega_k, N} = \hat{C}_{\hat{\phi}_N(\omega_k), N}$ obtained for the different ω_k 's are plotted in Fig. 6. A rapid inspection of

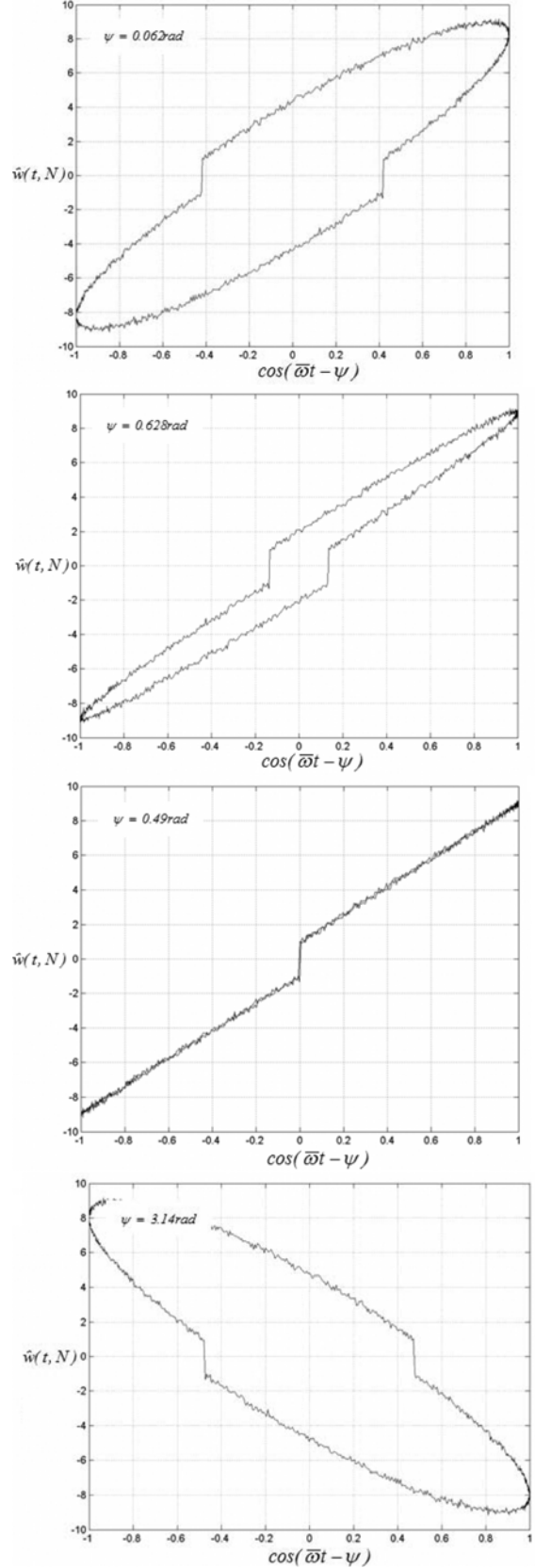


Fig. 5. Curves $C_{\psi, N}$ obtained with $\omega_1 = 0.2\pi$ rad/s and $N = 30$ for several values of ψ (simulation of Section IV-D-I).

these curves shows that the less spread (most concentrated) one of them is that corresponding to $\bar{\omega} = \omega_1 = 0.2\pi$ rad. Following Section IV-B, we will focus on the particular models

TABLE I
NUMERICAL VALUES OBTAINED IN SIMULATION OF SECTION IV-D-I

k	1	2	3	4	5	6
U_k	2	2	2	2	2	2
ω_k (rad/s)	0.2π	0.8π	π	1.6π	2π	2.5π
$ \overline{G}(j\omega_k) $	0.5	0.466	0.449	0.392	0.355	0.314
$-\angle\overline{G}(j\omega_k)$ (rad)	0.494	1.730	2.034	2.699	2.999	3.276
$\hat{\phi}_N(\omega_k)$ (rad)	0.490	1.734	2.026	2.689	2.990	3.275
$ \hat{G}(j\omega_k) $	0.505	0.470	0.455	0.400	0.365	0.320

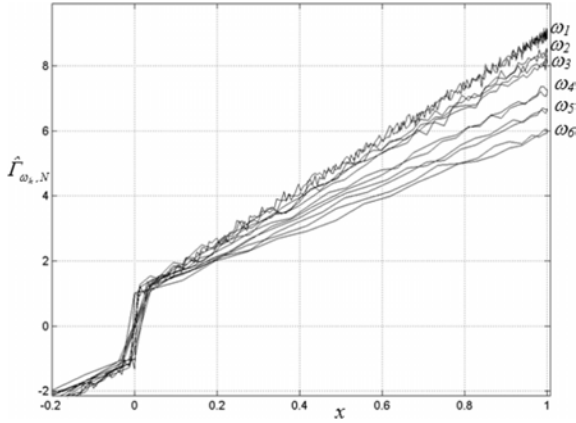


Fig. 6. Curves $\hat{\Gamma}_{\omega_k, N} \stackrel{def}{=} \hat{C}_{\hat{\phi}_N(\omega_k), N}$ obtained for the frequencies ω_k ($k = 1, \dots, 6$) (simulation of Section IV-D-I).

$(\overline{G}(s), \overline{f}(x))$ and $(\overline{G}^-(s), \overline{f}^-(x))$, defined by (34)–(35) which, presently, are characterized by:

$$G(s) = \frac{4}{7.96} \frac{(1 - \frac{s}{\pi})}{(1 + \frac{s}{\pi})(1 + \frac{0.5s}{\pi})}$$

$$\overline{f}(x) = \text{sign}(x) (\text{abs}(7.96x) + 1)$$

and $(\overline{G}^-(s), \overline{f}^-(x)) = (-\overline{G}(s), \overline{f}(-x))$. According to the estimation procedure NLE1–NLE4, the nonlinearity estimate \hat{f}_N is defined by the particular static curve $\hat{\Gamma}_{\omega_k, N} \stackrel{def}{=} \hat{C}_{\hat{\phi}_N(\omega_k), N}$. It is easily checked that, for this example, \hat{f}_N coincides with \overline{f} . The compatibility between the phase estimates, on one hand, and the nonlinearity estimate, on the other hand, is thus guaranteed just as this was predicted by Theorem 4.2. Recall that, in practical situations, it does not really matter which model, $(\overline{G}(s), \overline{f}(x))$ or $(\overline{G}^-(s), \overline{f}^-(x))$, is actually being identified.

Given the estimates $\hat{\phi}_N(\omega_k)$ and \hat{f}_N , the estimator (43a-c) is resorted to get estimates $|\hat{G}(j\omega_k)|$ of the frequency gains $|\overline{G}(j\omega_k)|$. This is illustrated by Fig. 7 which shows the cost function $J_{k, N}(\alpha)$ plotted against $\alpha \in [0, (1/U_3)]$ for $\omega_3 = \pi$ rad, $U_3 = 2$. It is seen that the global minimum is achieved for $\alpha = |\hat{G}(j\omega_3)| = 0.455$ which is very close to the true gain value. Table I gives the gain estimates thus obtained for different frequencies and shows that the quality of estimation is

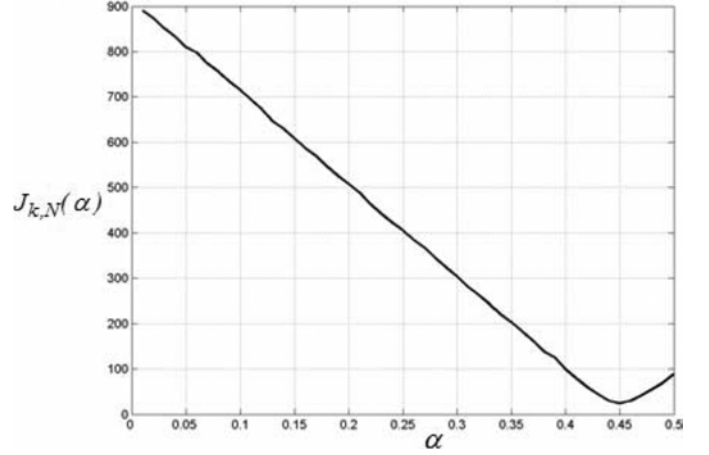


Fig. 7. Plot of $J_{k, N}(\alpha)$ for $\omega_3 = \pi$ rad (simulation of Section IV-D-I).

quite satisfactory. Hence, the consistency of the whole identification method is confirmed, despite the presence of significant noise amplitude (Fig. 4) and nonlinearity discontinuity (44b).

2) *Identification of Non-Invertible Nonlinearity:* In this subsection we only focus on phase estimation for a specific Wiener system involving a not invertible nonlinearity. By the way, it will be shown, using the considered example, that the method proposed in [1] is unable to recover the true value (modulo π) of the phase, while our method will be able to do it. The considered Wiener system is characterized by

$$G(s) = \frac{10}{(\frac{1.2}{\pi}s + 1)^4} \text{ and } f(x) = -x^2. \quad (45)$$

The system output is disturbed by a zero-mean noise $v(t)$ that is randomly uniformly distributed in $[-0.5, +0.5]$.

As $f(x)$ is even, it follows from Assumption A1 (part a) that $f(0)$ must be known. That is, the fact that $f(0) = 0$ can be used in the identification process. First, the phase estimator GPE1–GPE4 is applied to get an estimate of the phase $\varphi(\omega) \stackrel{def}{=} -\angle G(j\omega)$ for $\omega = \pi$ rad/s. To this end, the system is excited by the signal $u(t) = 2\cos(\omega t)$. Fig. 8 shows the closed-locus $\hat{C}_{\psi, N}$ obtained with different values of ψ and $N = 30$. According to GPE1–GPE4, the phase estimate $\hat{\phi}_N(\omega)$ is that value of ψ that leads to a static curve. Inspecting Fig. 8, it is readily seen that there are two possible values for $\hat{\phi}_N(\omega)$, namely $\psi_1^* = 0.3612$ rad and $\psi_2^* = 1.9321$ rad. The second value is discarded as it leads to a nonadmissible nonlinearity because then $f(0) \neq 0$. Therefore, we let $\hat{\phi}_N(\omega) = 0.3612$ rad. As the true value of the phase is $\varphi(\omega) = -4 \tan^{-1}(1.2) = -3.5042$ rad it follows that $\varphi(\omega) - \hat{\phi}_N(\omega) \cong \pi$ i.e., $\hat{\phi}_N(\omega)$ equals $\varphi(\omega)$ modulo π . Hence, the obtained phase estimate is consistent. The corresponding static curve $\hat{\Gamma}_{\omega, N} \stackrel{def}{=} \hat{C}_{\hat{\phi}_N(\omega), N}$ then gives the estimate \hat{f}_N which presently corresponds to $f^-(x) = f(-x)$. But, as f is even, one has $f(-x) = f(x)$.

Let us now apply the method proposed in [1] to get a phase estimate for the same frequency i.e., $\omega = \pi$ rad. Accordingly, the estimate of $\varphi(\omega) \stackrel{def}{=} -\angle G(j\omega)$ is given by the rule

$$\hat{\Phi}(\omega) = -\frac{1}{i} \tan^{-1} \left(\frac{\text{Im}(Y(i\omega))}{\text{Re}(Y(i\omega))} \right)$$

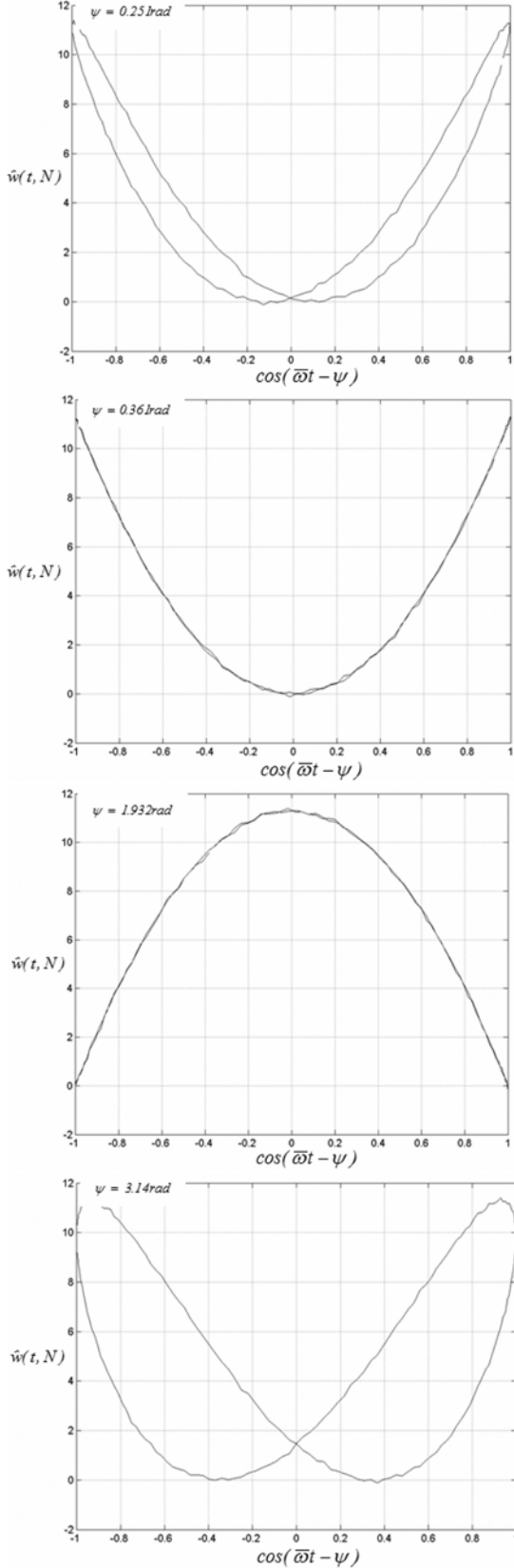


Fig. 8. Curves $C_{\psi, N}$ obtained for several values of ψ (simulation of Section IV-D-II).

where Y denotes the Fourier (Discrete) Transform of a filtered and sampled version of the system output signal $y(t)$ and i is any integer (generally the first one) such that $Y(i\omega) \neq 0$. In the present case

$$\begin{aligned} y(t) = x(t)^2 &= -\frac{1}{2} - \frac{1}{2} \cos(2\omega t - 7.008) \\ &= -\frac{1}{2} - \frac{1}{2} \cos(2\omega t - 0.725) \end{aligned}$$

where the noise effect has been ignored for simplicity and also there is no need to signal filtering and sampling. This clearly shows that the unique possible choice of the integer i is $i = 2$. Furthermore, it is readily seen that $Y(2\omega) = -0.25e^{-j0.725} = 0.25e^{j(\pi-0.725)}$ which implies the following phase estimate:

$$\begin{aligned} \hat{\Phi}(\omega) &= -\frac{1}{2} \tan^{-1} \left(\frac{\text{Im}(Y(2\omega))}{\text{Re}(Y(2\omega))} \right) = -\frac{1}{2}(\pi - 0.725) \\ &= -1.208 \text{ rad.} \end{aligned}$$

It is readily seen that $\hat{\Phi}(\omega) - \varphi(\omega) = -1.208 + 3.5042 = 0.7308 \times \pi$ rad. This is clearly different from zero (modulo π). The phase estimate is thus biased. This counter example shows that the phase estimator obtained using the approach proposed in [1], is not consistent in all situations. Consequently, the nonlinearity and the frequency gains cannot be consistently estimated based on such phase estimator, see [2] for more details.

V. PRACTICAL ISSUES

A. Useful Analytical Expressions

1) *Analytical Evaluation of the Geometric Area:* Let $A(\psi, N)$ denote the geometric area of the curve $\hat{C}_{\psi, N}$. It follows using Proposition 3.2 and (9), that:

$$\begin{aligned} A(\psi, N) &= \int_0^T \left| \hat{w} \left(T - t + 2\frac{\psi}{\omega}, N \right) - \hat{w}(t, N) \right| \left| \frac{dx_{\psi}}{dt} \right| dt \\ &= \frac{2\pi}{T} \int_0^T \left| \hat{w} \left(T - t + 2\frac{\psi}{\omega}, N \right) - \hat{w}(t, N) \right| \\ &\quad \times |\sin(\omega t - \psi)| dt. \end{aligned} \quad (46)$$

This provides us with an analytical rule for static feature recognition, namely $\hat{C}_{\psi, N}$ is static if $A(\psi, N) = 0$. Now, using Proposition 3.5 it follows that if $A(\psi, N) = 0$ (for a sufficiently large value of N) then, one has either $\psi = \varphi(\omega)$ or $\psi = \varphi(\omega) + \pi$. In the first case, the mapping $\cos(\omega t - \psi) \rightarrow \hat{w}(t, N)$ gives an estimate \hat{f}_N of f otherwise the mapping corresponds to f^- . The smaller $A(\psi, N)$ the better the estimation quality is. Procedure GPE1-GPE4 can then be reformulated as a problem of optimizing the nonlinear function $A(\psi, N)$. As the problem is one-dimensional and the domain search is *well defined* (namely $[0, \pi]$), the minimum can be determined graphically. To illustrate this analytical way by simulation, consider the simulation conditions of Section IV-D-I. Let us focus the illustration on $\omega = 0.2\pi$ rad. The corresponding function $A(\psi, N)$ is plotted versus ψ in Fig. 9(a). It is seen that $A(\psi, N)$ actually has a global minimum ψ^* in the interval $[0, \pi)$. Specifically, $\psi^* = 0.492$ rad, and this is precisely the value obtained in Section IV-D-I.

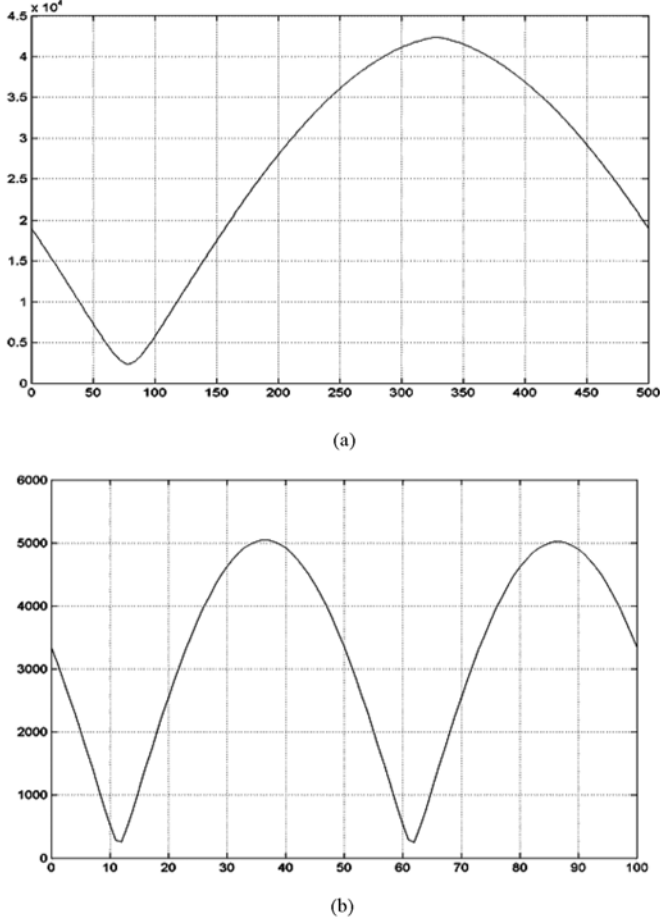


Fig. 9. (a) Plot of $A(\psi, N)$ vs ψ , for $0 \leq \psi < \pi$ for the Wiener system of Section IV-D-I. (b) Plot of vs $A(\psi, N)$ vs ψ , for $0 \leq \psi < \pi$ for the Wiener system of Section IV-D-II.

Now, let us consider the Wiener system of Section IV-D-II, which involves a noninvertible nonlinearity. We aim at estimating the phase for $\omega = \pi$ rad/s. The corresponding function $A(\psi, N)$ is represented (versus ψ) in Fig. 9(b). It is seen that $A(\psi, N)$ actually has a global minimum in the interval $[0, \pi)$. This is achieved at $\psi^* \approx 0.367$ rad which is very close to the phase estimate obtained earlier in Section IV-D-II.

2) *Analytical Evaluation of Signal Spread*: Let us consider the family of (static) curves $\hat{\Gamma}_{\omega, N} \stackrel{def}{=} \hat{C}_{\hat{\phi}_N(\omega), N}$, $(U, \omega) \in \{(U_1, \omega_1), \dots, (U_m, \omega_m)\}$, constructed in GPE1–GPE4. Let $g_k(x)$ ($-1 \leq x \leq 1$) denote the function induced by the static curve $\hat{\Gamma}_{\omega_k, N}$. It was noticed in Section IV-B that each function $g_k(x)$ is a more or less spread version of the functions f or f^- . According to the estimation procedure NLE1–NLE4, the estimate of the nonlinearity is that function $g_k(x)$ that presents the smallest degree of spread. Doing so, one recovers the largest part of the system nonlinearity (f or f^-). In the simulation of Section IV-D-I, this was easily recognized using the plots of $\hat{\Gamma}_{\omega_k, N}$ (Fig. 6). The spread degree can also be evaluated analytically using the following measure ([4]):

$$S_k = \frac{\int_{-1}^{+1} x^2 |g_k(x)|^2 dx}{\int_{-1}^{+1} |g_k(x)|^2 dx}. \quad (47)$$

The larger S_k the more spread is the function $g_k(x)$. According to the procedure NLE1–NLE4, the best estimate for the system nonlinearity is that function $g_k(x)$ with the smallest value of S_k .

B. Practical Implementation Issues

The implementation of the proposed identification method can only be performed with digital means. This necessitates signal sampling and numerical approximations of involved mathematical expressions.

1) *Signal Sampling and Noise Effect*: Input signal sampling is easily handled as the used signals are sinusoidal. The output signal is a periodic signal (with period $T = 2\pi/\omega$) corrupted with noise i.e., $y(t) = w(t) + v(t)$. Nevertheless, the noise effect is readily filtered thanks to the averaging (29). Indeed, it is seen from Proposition 3.5 (Part 1) that the average output, namely $\hat{w}(t, N)$, does converge in probability to $w(t)$ whatever t . This particularly holds for $w(t)$ at the sampling time instants $t = kT_s$ ($k = 0, 1, 2, \dots$) where T_s denotes the sampling period which, presently, is chosen of the form $T_s = (T/M) = (2\pi/M\omega)$ for some integer $M \gg 1$. Furthermore, the averaging (29) is an algebraic operation that is easily realisable using digital means.

The consistency of $\hat{w}(t, N)$ implies that related sampling issue is equivalent to the sampling of $w(t)$. As this is a periodic signal it can be approximated by $w(t) \approx w_L(t) \stackrel{def}{=} \sum_{n=-L}^{+L} W_n e^{jn\omega t}$ (the W_n 's denote its Fourier coefficients). The sampling period should satisfy the Shannon condition $(1/T_s) \geq 2(L\omega/2\pi)$ or, equivalently, $M \geq 2L$. That is, the number M of samples in the time interval $[0, T]$ must be at least twice the number N of selected harmonics.

Remark 5.1: A similar discussion of periodic signal sampling is made in [1]. More elaborate results on periodic signals sampling can be found in [21] and reference list therein.

2) *Numerical Version of the Phase Estimation Part*: For digital implementation purpose, a numerical version has to be developed for the identification method. While algebraic expressions are digitally implemented just substituting sampled data to continuous signals, the implementation of integral expressions relies on numerical approximations (like rectangle or trapezoidal methods). In the rest of this subsection, we will focus on developing a numerical version for the phase estimation part (GPE1–GPE4). The other identification method parts (nonlinearity and frequency gain modulus) can be handled similarly.

First, the $L_2[0, T]$ norms involved in the step GPE2 are approximated as in usual practice, e.g.

$$\|\hat{w}(N)\|_{2d} = \left(T_s \sum_{k=0}^{M-1} \hat{w}(kT_s, N)^2 \right)^{1/2}.$$

Then, step GPE3 should read: 'Plot the (closed) parameterized curve $\hat{C}_{\psi, N, M} \stackrel{def}{=} \{(\cos(\omega kT_s - \psi), \hat{w}(kT_s, N)), k = 0, \dots, M-1\}$ with $M = T/T_s$ '. As the sampling time kT_s is substituted to the continuous-time t , the obtained curve, $\hat{C}_{\psi, N, M}$, is no longer a continuous line. Nevertheless, the consistency of the

discrete curve $\hat{C}_{\psi, N, M}$ is still guaranteed because $\hat{w}(kT_s, N)$ is consistent. Specifically, one has w.p.1, for all k

$$\begin{aligned} & (\cos(\omega kT_s - \psi), \hat{w}(kT_s, N)) \\ & \xrightarrow{N \rightarrow \infty} (\cos(\omega kT_s - \psi), w(kT_s)). \end{aligned}$$

The phase estimate obtained in step GPE3 is then denoted $\hat{\phi}_{N, M}(\omega)$ and its quality depends partly on the accuracy with which the discrete curve $\{(\cos(\omega kT_s - \psi), \hat{w}(kT_s, N)), k = 0, \dots, M-1\}$ approximates the continuous line $\{(\cos(\omega t - \psi), \hat{w}(t, N)), 0 \leq t \leq T\}$. It is clear that, $\{\hat{w}(kT_s, N); k = 0, \dots, M-1\}$ tends to $\{\hat{w}(t, N); 0 \leq t \leq T\}$ when $M \rightarrow \infty$ (i.e., when $T_s \rightarrow 0$). Then, the result of Proposition 3.5 (Part 4) guarantees that $\hat{\phi}_{N, M}(\omega) \xrightarrow{N, M \rightarrow \infty} \phi(\omega)$ or $\phi(\omega) + \pi$.

Step GPE4 applies exactly as in the continuous-time case.

Now, let us go back to step GPE3 which involves static curve recognition. It has been pointed out (Section V-A-I) that such recognition can be performed using expression (46) to evaluate the geometric area $A_d(\psi, N)$ of the curve. The numerical version of such expression is

$$A_d(\psi, N, M) = \frac{2\pi T_s}{T} \sum_{k=0}^{M-1} \left| \hat{w} \left(T - kT_s + 2\frac{\psi}{\omega}, N \right) - \hat{w}(kT_s, N) \right| |\sin(\omega kT_s - \psi)|. \quad (46a)$$

Note that the time $T - kT_s + 2(\psi/\omega)$ in the right side of (46) must be a multiple of the sampling period T_s . As $T = MT_s$ and $\omega = 2\pi/T$, one readily gets that $T - kT_s + 2(\psi/\omega) = (M - k + (\psi M/\pi))T_s$. This suggests that ψ should be of the form $\psi = m(\pi/M)$ (m being integer). Doing so, the problem at hand turns out to be the minimization of the quantity $A_d(m(\pi/M), N, M)$ with respect to m . The minimum search can be performed graphically as explained in Section V-A-I. According to the step GPE3, such minimization task determines the true phase $\phi(\omega)$ (modulo π) up to an error bounded by π/M . That is, the larger the number M of data samples the better the phase estimation accuracy is.

VI. CONCLUSION

In this paper, a frequency-domain solution has been developed to deal with Wiener system identification. Unlike most previous works, the system nonlinearity is not necessarily required to be (globally) invertible and smooth. The main component of the proposed identification method is the consistent phase estimator GPE1-GPE4 described in Section IV-A. The design of this estimator essentially relays on the geometric findings of Section III which are original features of this work. The main outcome of such investigation is that the Lissajous curves C_ψ

are all nonstatic except for $\psi = \varphi + k\pi$. Inversely, when C_ψ is static then it corresponds to $f(\cdot)$ or to $f^-(\cdot)$ or to (more or less) spread versions of these. The focus has been made on the couple of models $(M(\bar{U}, \bar{w}), M^-(\bar{U}, \bar{w}))$ that involve the less spread (i.e., most condensed) nonlinearities. This choice has proved to be judicious in regard to gain estimation. The fact that the nonlinearity estimation is coupled with the phase estimation guarantees the compatibility of the corresponding estimates. The above compatibility and spread facts are new features in this work.

REFERENCES

- [1] E. W. Bai, "Frequency domain identification of Wiener models," *Automatica*, vol. 39, pp. 1521–1530, 2003.
- [2] F. Giri, Y. Rochdi, and F. Z. Chaoui, "Comment on 'frequency domain identification of Wiener models'," *Automatica*, vol. 44, pp. 1451–1455, 2008.
- [3] J. Bruls, C. T. Chou, B. R. J. Heverkamp, and M. Verhaegen, "Linear and nonlinear system identification using separable least squares," *Eur. J. Control*, vol. 5, pp. 116–128, 1999.
- [4] M. Carbon, D. Ghorbanzadeh, P. Marry, N. Point, and D. Vial, *Mathematical Elements for Signals*. Paris, France: Dunod, 1997.
- [5] H. F. Chen, "Recursive identification for Wiener model with discontinuous piece-wise linear function," *IEEE Trans. Automat. Control*, vol. 51, no. 3, pp. 390–400, Mar. 2006.
- [6] A. Gardiner, "Frequency domain identification of nonlinear systems," in *Proc. IFAC Symp. Syst. Ident. Estim.*, Rotterdam, The Netherlands, 1993, pp. 831–834.
- [7] W. Greblicki, "Nonparametric identification of Wiener systems," *IEEE Trans. Inform. Theory*, vol. 38, no. 5, pp. 1487–1493, Sep. 1992.
- [8] W. Greblicki, "Nonparametric approach to Wiener system identification," *IEEE Trans. Circuits Syst. I*, vol. 44, no. 6, pp. 538–545, Jun. 1997.
- [9] W. Greblicki, "Recursive identification of Wiener system," *Appl. Math. Comput. Sci.*, vol. 11, pp. 977–991, 2001.
- [10] W. Greblicki, "Nonlinearity recovering in Wiener system driven with correlated signal," *IEEE Trans. Automat. Control*, vol. 49, no. 10, pp. 1805–1810, Oct. 2004.
- [11] Z. Hasiewicz, "On equivalence conditions of local and global identification of a memoryless cascade complex system," *Syst. Anal. Model. Simul.*, vol. 4, pp. 341–345, 1987.
- [12] X. L. Hu and H. F. Chen, "Strong consistency of recursive identification for Wiener systems," *Automatica*, vol. 41, pp. 1905–1916, 2005.
- [13] I. W. Hunter and M. J. Korenberg, "The identification of nonlinear biological systems: Wiener and Hammerstein cascade models," *Biol. Cybern.*, vol. 55, pp. 135–144, 1986.
- [14] A. E. Nordström and L. H. Zetterberg, "Identification of certain time-varying nonlinear Wiener and Hammerstein systems," *IEEE Trans. Signal Processing*, vol. 49, no. 3, pp. 577–592, May 2001.
- [15] G. A. Pajunen, "Adaptive control of Wiener type nonlinear systems," *Automatica*, vol. 28, pp. 781–785, 1992.
- [16] M. Pawlak, Z. Hasiewicz, and P. Wachel, "On nonparametric identification of Wiener systems," *IEEE Trans. Signal Processing*, vol. 55, no. 2, pp. 482–492, Feb. 2007.
- [17] J. Vörös, "Parameter identification of Wiener systems with discontinuous nonlinearities," *Syst. Control Lett.*, vol. 44, pp. 363–372, 2001.
- [18] E. W. Weisstein, "Lissajous Curve," MathWorld, a Wolfram Web Resource, Tech. Rep. [Online]. Available: <http://mathworld.wolfram.com/LissajousCurve.html>
- [19] D. T. Westwick and R. E. Kearney, "A new algorithm for the identification of multiple-input Wiener systems," *Biol. Cybern.*, vol. 68, pp. 75–85, 1992.
- [20] T. Wigren, "Recursive prediction error identification using the nonlinear Wiener model," *Automatica*, vol. 29, pp. 1011–1025, 1993.
- [21] M. Jacob, T. Blu, and M. Unser, "Sampling of periodic signals: A quantitative error analysis," *IEEE Trans. Signal Processing*, vol. 50, no. 5, pp. 1153–1159, May 2002.